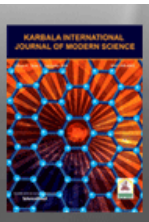
Karbala International Journal of Modern Science

Manuscript 3279

Fano-type resonance structures based on combination of fiber Bragg grating with Fabry-Perot interferometer

A.Zh. Sakhabutdinov

T.A. Agliullin

S.M.R.H. Hussein

A.A. Kuznetsov

V.I. Anfinogentov

See next page for additional authors

Fano-type resonance structures based on combination of fiber Bragg grating with Fabry-Perot interferometer

Abstract

The work is dedicated to the mathematical modeling of the combined fiber-optic structure, which consists of a Fabry-Perot interferometer in the form of a thin polymer film at the end of an optical fiber and a fiber Bragg grating formed near it. The simulation results obtained using the proposed rigorous mathematical model are in good agreement with the reflectance spectrum of the experimental fiber-optic structure. It is shown that the combination of two resonant wave processes in the optical fiber leads to the asymmetric Fano-type resonance. The spectral shape of the resonance depends on the parameters of the structure, in particular, on the permittivity and the permeability of the constituting media, the thickness of the Fabry-Perot resonator, the length of the fiber Bragg grating, its induced refractive index and the period, as well as on temperature and humidity. The prospects of using the asymmetric resonance effect of the combined structure in sensing applications are discussed.

Keywords

combined fiber-optic sensor, fiber Bragg grating, FabryPerot interferometer, mathematical model of combined fiber optic sensors, gas concentration sensor, asymmetrical resonance, Fano resonance

Authors

A.Zh. Sakhabutdinov, T.A. Agliullin, S.M.R.H. Hussein, A.A. Kuznetsov, V.I. Anfinogentov, and B.I. Valeev

RESEARCH PAPER

Fano-Type Resonance Structures Based on Combination of Fiber Bragg Grating with Fabry-Perot Interferometer

A.Zh. Sakhabutdinov [a,*], T.A. Agliullin [a], S.M.R.H. Hussein [b], A.A. Kuznetsov [a], V.I. Anfinogentov [a], B.I. Valeev [a]

[a] Kazan National Research Technical University named after A.N.Tupolev-KAI, 10, K. Marx str., 420011, Kazan, Russian Federation
[b] University of Karbala, Karbala, 56001, Iraq

Abstract

The work is dedicated to the mathematical modeling of the combined fiber-optic structure, which consists of a Fabry-Perot interferometer in the form of a thin polymer film at the end of an optical fiber and a fiber Bragg grating formed near it. The simulation results obtained using the proposed rigorous mathematical model are in good agreement with the reflectance spectrum of the experimental fiber-optic structure. It is shown that the combination of two resonant wave processes in the optical fiber leads to the asymmetric Fano-type resonance. The spectral shape of the resonance depends on the parameters of the structure, in particular, on the permittivity and the permeability of the constituting media, the thickness of the Fabry-Perot resonator, the length of the fiber Bragg grating, its induced refractive index and the period, as well as on temperature and humidity. The prospects of using the asymmetric resonance effect of the combined structure in sensing applications are discussed.

Keywords: Combined fiber-optic sensor, Fiber bragg grating, Fabry-perot interferometer, Mathematical model of combined fiber optic sensors, Gas concentration sensor, Asymmetrical resonance, Fano resonance

1. Introduction

Progress in photonics and nanotechnology is based mainly on resonant optical phenomena related to nature and physics of light [1]. Noticeable achievements in fiber-optic measurement systems are based on sensing elements implemented using Fabry-Perot resonators [2—4], photonic crystals [5—7] or fiber Bragg gratings [8,9]. In some cases, the quality factor of the resonance is insufficient, and one has to resort to techniques to narrow the frequency range of the resonance region. A fiber Bragg grating with a discrete phase π-shift is one of the examples of such techniques [10—12]. The fiber Bragg grating with a discrete phase π-shift can be presented as a combination of three uniform elements — two Bragg fiber gratings and a Fabry-Perot cavity between them. Recently, the number of research works dedicated to the effects associated with the physics of Fano resonances [13—17] and their applications in optical communication and sensing has increased greatly. For the successful design, it is important not only to obtain the Fano resonance in fiber optics, but also to understand its nature. The Fano resonance is a special type of resonance with an asymmetric frequency response, it is the result of two wave processes interference. The Fano resonance in fiber-optic structures has been obtained and studied by Carlo Edoardo Campanella et al. [13,18,19], Iwao Teraoka [20], Kathleen McGarvey-Lechable [21], Síle Nic Chormaic [22], Fang Chen [23]. The main effect was

Received 1 November 2022; revised 27 November 2022; accepted 1 December 2022.
Available online 13 January 2023

* Corresponding author at. Kazan National Research Technical University named after A.N.Tupolev-KAI, 10, K. Marx str., 420011, Kazan, Russian Federation.
E-mail address: azhsakhabutdinov@kai.ru (A.Zh. Sakhabutdinov).

https://doi.org/10.33640/2405-609X.3279

obtained from the interference of two resonances — the Bragg resonance on a multilayer periodic structure (fiber Bragg grating) and the resonance on the optical micro-ring resonator [18,20,24,25]. The wave mixing from two resonators in the suggested form may cause certain manufacturing difficulties due to the small (3–5 μm) diameter of the ring.

Another solution to obtain asymmetric Fano resonance was found during the research and design of *the combined fiber-optic sensor* (CFOS). The CFOS was designed for simultaneous measurement of gas concentration and environmental temperature. The CFOS is the sequential combination of *the fiber Bragg grating* (FBG) and *the Fabry-Perot resonator* (FPR) [26–28]. The asymmetric Fano-type resonance in this case is the result of optical mixing of two wave processes with different resonance frequencies, namely the Bragg and the Fabry-Perot resonances, with optical radiation acting as forcing oscillation.

As it has been shown in [28], a sensitive structure suitable for environmental monitoring consists of an FPR in the form of a thin film at the end face of the optical fiber with the FBG near it. The film refractive index varies depending on the gas concentration in the environment. The spectral response of the FPR is sensitive to various environmental parameters, particularly to temperature and gas concentration. The FBG spectrum mainly depends on temperature, while variations of other environmental parameters have no significant influence on it. Thus, simultaneous measurement of temperature and gas concentration is achievable using CFOS. The CFOS architecture serves as an effective single-point measurement method, moreover, it has a great potential for CFOS multiplexing in arrays.

Despite a vast amount of research dedicated to the development of combined sensors based on an FBG and an FPR, most of the works do not consider distortions in the FBG spectrum that can occur in such sensors. The evidence of this effect can be found in [29], where the transmission notch can be observed near the reflection peak of the FBG spectrum. Therefore, the resulting spectrum of the CFOS cannot be represented as a simple sum of reflectance spectra of the constituent elements — the FBG and the FPR.

2. Modeling and experimental results

The reflectance spectrum of the CFOS can be estimated using mathematical modeling based on the transfer-matrix method [30,31]. According to this method, the structure of CFOS is divided into three uniform sections: FBG, FPR, and the gas environment, as shown in Fig. 1. For each section, the reflectance and transmittance are determined for the co- and counter-directed wave modes passing through it [31].

The transfer matrix of the FBG is determined according to the coupled mode theory and is formulated as:

$$\mathbf{T}_{\mathrm{FBG}}(\lambda, n, \Delta n, \Lambda, H) = \begin{bmatrix} T_{11} & T_{12} \\ T_{22} & T_{22} \end{bmatrix}, \tag{1}$$

where T_{ij} are defined as:

$$\begin{aligned} T_{11} = \overline{T}_{22} &= \cosh(\gamma \cdot H) - j\frac{\Delta\beta}{\gamma}\sinh(\gamma \cdot H) \ , T_{12} \\ &= \overline{T}_{21} = -j\frac{\kappa}{\gamma}\sinh(\gamma \cdot H), \end{aligned} \tag{2}$$

where H is the FBG length. The parameters $\kappa(\lambda)$, $\Delta\beta(\lambda)$, and $\gamma(\lambda)$ in (1) are defined as follows:

$$\begin{aligned} \kappa(\lambda) = \pi\frac{\Delta n}{2\lambda}, \Delta\beta(\lambda) = \frac{\pi}{\Lambda} - \pi\frac{2n + \Delta n}{\lambda}, \\ \gamma(\lambda) = \sqrt{|\kappa(\lambda)|^2 - \Delta\beta(\lambda)^2}, \end{aligned} \tag{3}$$

where Λ is the period of the FBG, n is the refractive index of the fiber core, Δn is the induced refractive index, λ is the wavelength.

The Fabry-Perot resonator is modeled using the set of three scattering matrices. The first and the third ones are the matrices of the rapid change in propagation medium parameters (interface between fiber and polymer; interface between polymer and environment, in Fig. 1). The second one is the matrix of the homogeneous inner medium of the resonator cavity (Polymer film, Fig. 1).

The scattering matrix of the homogeneous inner medium of the FPR cavity is formulated as:

$$\mathbf{S}_{\mathrm{M}}(\lambda, \epsilon, \mu, h) = \begin{bmatrix} 0 & e^{-j\cdot h\cdot\frac{\pi}{\lambda}\cdot\gamma(\epsilon,\mu)} \\ e^{-j\cdot h\cdot\frac{\pi}{\lambda}\cdot\gamma(\epsilon,\mu)} & 0 \end{bmatrix}, \tag{4}$$

where h is the medium thickness, and $\gamma(\epsilon, \mu)$ is defined as follows:

$$\begin{aligned} \gamma(\epsilon, \mu) = \sqrt{2\mathrm{Re}\epsilon\cdot\mathrm{Re}\mu} \times \\ \times\left(\sqrt{\sqrt{1 - \left(\frac{\mathrm{Im}\epsilon}{\mathrm{Re}\epsilon}\right)^2} + 1} - j\sqrt{\sqrt{1 - \left(\frac{\mathrm{Im}\epsilon}{\mathrm{Re}\epsilon}\right)^2} - 1}\right), \end{aligned} \tag{5}$$

where ϵ and μ are permittivity and permeability of the medium.

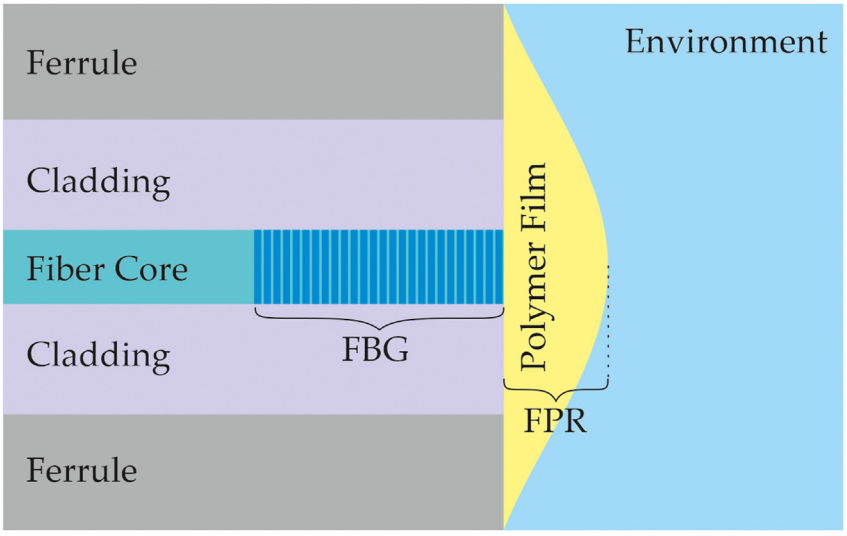

Fig. 1. The sensitive element of the CFOS.

The scattering matrix of the rapid change in propagation medium parameters is formulated according to:

$$\mathbf{S}_{\mathrm{J}}(\epsilon_1,\mu_1,\epsilon_2,\mu_2,)=\begin{bmatrix}\frac{\sqrt{\epsilon_1\mu_2}-\sqrt{\mu_1\epsilon_2}}{\sqrt{\mu_1\epsilon_2}+\sqrt{\epsilon_1\mu_2}} & \frac{2\cdot\sqrt[4]{\epsilon_1\mu_1\epsilon_2\mu_2}}{\sqrt{\mu_1\epsilon_p}+\sqrt{\epsilon_1\mu_2}}\\ \frac{2\cdot\sqrt[4]{\epsilon_1\mu_1\epsilon_2\mu_2}}{\sqrt{\mu_1\epsilon_2}+\sqrt{\epsilon_1\mu_2}} & \frac{\sqrt{\mu_1\epsilon_2}-\sqrt{\epsilon_1\mu_2}}{\sqrt{\mu_1\epsilon_2}+\sqrt{\epsilon_1\mu_2}}\end{bmatrix}, \tag{6}$$

written for two different mediums with two parameter sets (ϵ_1, μ_1 — the permittivity and permeability of the source media and ϵ_2, μ_2 — the same parameters of the destination media).

Each transfer matrix corresponds to its scattering matrix by the formula:

$$\mathbf{T}(\mathbf{S})=\frac{1}{S_{2,1}}\begin{pmatrix}S_{2,1}S_{1,2}-S_{1,1}S_{2,2} & S_{1,1}\\ -S_{2,2} & 1\end{pmatrix} \tag{7}$$

The resulting transfer matrix of the CFOS structure (FBG with FPR) is the product of the transfer matrices of its components:

$$\mathbf{T}(\lambda)=\mathbf{T}_{\mathrm{FBG}}(\lambda,n,\Delta n,\Lambda,H)\times\mathbf{T}\left(\mathbf{S}_{\mathrm{J}}\left(\epsilon_{\mathrm{f}},\mu_{\mathrm{f}},\epsilon_{\mathrm{p}},\mu_{\mathrm{p}}\right)\right)\times \times\mathbf{T}\left(\mathbf{S}_{\mathrm{M}}\left(\lambda,\epsilon_{\mathrm{p}},\mu_{\mathrm{p}},h\right)\right)\times\mathbf{T}\left(\mathbf{S}_{\mathrm{J}}\left(\epsilon_{\mathrm{p}},\mu_{\mathrm{p}},\epsilon_{\mathrm{g}},\mu_{\mathrm{g}}\right)\right), \tag{8}$$

where ϵ_f, μ_f, ϵ_p, μ_p and ϵ_g, μ_g are the permittivity and permeability of the fiber core, the polymer (gas-sensitive film), and the gas environment sections of the structure, respectively.

The reverse transform of the transfer matrix to the scattering matrix is calculated according to:

$$\mathbf{S}(\mathbf{T}(\lambda))=\frac{1}{T_{2,2}}\begin{pmatrix}T_{1,2} & T_{1,1}T_{2,2}-T_{1,2}T_{2,1}\\ 1 & T_{2,1}\end{pmatrix} \tag{9}$$

The reflection ratio is a wavelength-dependent value which is equal to:

$$C(\lambda)=|S_{1,1}|^2 \tag{10}$$

The refractive index and the induced refractive index of the FBG, the FBG length, the FPR length, permittivity and permeability of all the media of the CFOS generally depend on temperature. In the mathematical model, it was captured by using the coefficient of thermal expansion and the thermo-optic coefficient. Considering the dependence of homogeneous section lengths and refractive indices on temperature was carried out according to the formulas:

$$l(T)=l_0(1+C_{\mathrm{TE}}\cdot(T-T_0)) \tag{11}$$

$$n(T)=n_0(1+C_{\mathrm{TO}}\cdot(T-T_0)) \tag{12}$$

where C_{TE} is the coefficient of thermal expansion, C_{TO} is the thermo-optic coefficient, T is the temperature, T_0 is the reference temperature, l_0 is the length and n_0 is the refractive index at $T = T_0$. The relationship between refractive index, permittivity and permeability is defined as $n^2 = \epsilon\cdot\mu$.

Using the approach presented above, numerical simulation of the CFOS spectrum was performed to compare it with the spectral response of the real-life sensor. The real-life sensor spectral response was obtained at the room temperature (22 °C) in the air environment. The comparing results are presented in Fig. 2, while the parameters of the CFOS model are listed in Table 1.

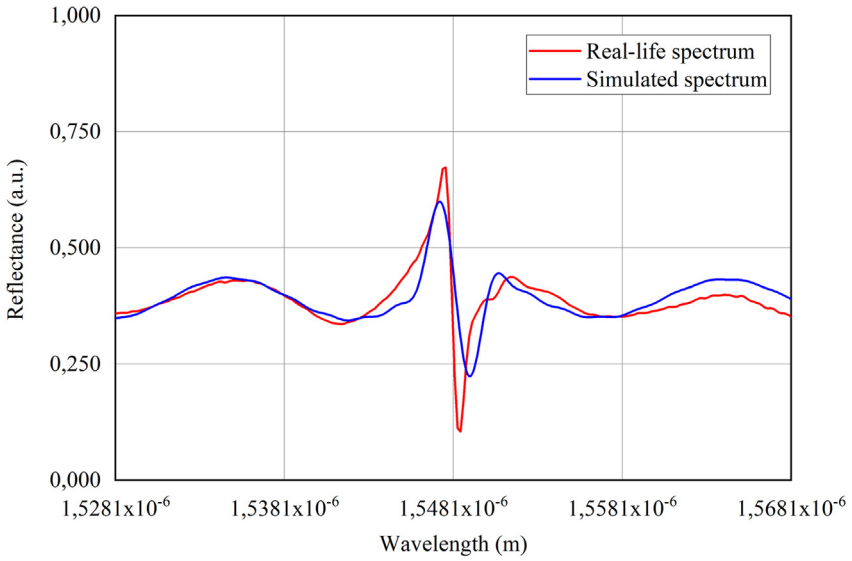

Fig. 2. Comparing results of simulated and real-life CFOS spectra: the real-life sensor — red line, the CFOS model — blue line.

Table 1. Parameters of CFOS.

Parameter	Value
Effective refractive index of the fiber core (n)	1.4586604
Induced refractive index of the FBG (Δn)	0.00027
FBG period (Λ, μm)	0.530612
FBG length (H, mm)	0.443
FPR permittivity/permeability (ϵ_p/μ_p)	2.226/1.0
FPR thickness (h, μm)	54.77
Environment permittivity/permeability (ϵ_g/μ_g)	1.0/1.0

As it can be seen at Fig. 2, the spectrum of the CFOS model estimated using the transfer matrix method has a good agreement with the experimental spectrum of the real-life CFOS. Both spectra include a narrow notch near the FBG reflectance peak, the spectral position of which coincides both for the experimental and the simulated spectra.

3. Discussion

The results allow us to state that the spectral form of this type of resonance has a larger number of degrees of freedom than the classical Fano resonance. At the same time, the physics and nature of the obtained resonance and the Fano resonance are similar, since both of them are the result of a superposition of two close resonance systems (FBG and Fabry-Perot cavity). Therefore, the resulting resonance is referred to as a Fano-type resonance.

We suppose that we managed not only to obtain the Fano-type resonance using the simple fiber-optic structure successfully, but also to describe it mathematically with consideration of all the CFOS specifics. It should be noted, that earlier we have encountered only a complicated description of the Fano-type resonance obtaining in fiber-optic structures [1,13,18–20,32–34]. Only in [35] we found similar forms of the spectral response, where the FBG with closed Fabry-Perot interferometer was investigated. Undoubtedly, it is useful to have an opportunity to study the evolution of the Fano-type resonance spectral response from CFOS, depending on the system parameters. The proposed mathematical model can be used for such study.

It should be noted that the relative shape of the asymmetric resonance spectrum depends on the wavelengths of the main resonances (Fabry-Perot and Bragg resonances). Fig. 3 shows three simulated spectra obtained with slightly different values of the CFOS parameters in comparison to Fig. 2. The FPR length is equal to 30 μm, the FBG length is equal to 5 mm, the refractive index of the Fabry-Perot layer is equal to 2.26. As a result of the simulations, three spectral responses with slightly different FBG period values were obtained. As it can be seen at Fig. 3, the FBG spectral shape and its narrow notch position depend on its position relative to the Fabry-Perot spectrum.

The configurations of the sensing structures that provide narrowband spectral components are of particular interest for the usage in measurement systems. Wavelength shifting of narrow notches with the slightest change in the structure configuration can provide high-resolution measurements in narrow ranges of varying parameters. For example, it can be used in high-precision measurements of temperature or refractive index (dielectric constant) of the FP layer.

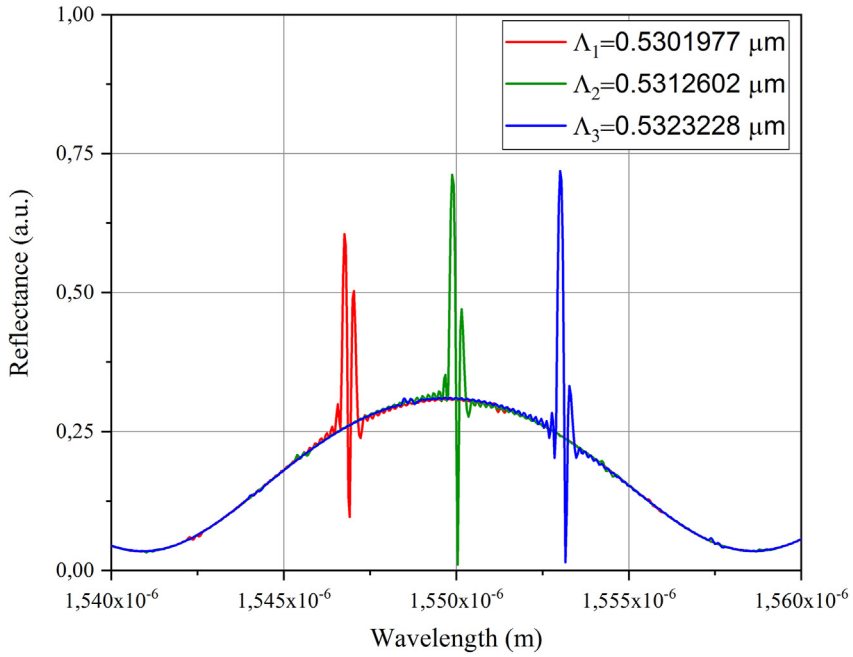

Fig. 3. Three CFOS spectra at different FBG periods.

From our point of view, the considered fiber-optic structures have the prospect of becoming highly sensitive transducers or signal level sensors. Assume that the sensor is implemented with the parameters that provide the spectral response with a narrowband transparency window adjacent to the FBG reflectance peak. The slightest change of the structure parameters will lead to noticeable change of the FBG spectrum, and the narrowband transparency window will fade away. Based on the analysis of the light intensity in the transparency window, a number of technically interesting solutions can be designed. The model parameters include the permittivity and permeability of all three media (optical fiber, polymer film, and environment), the period, the induced refractive index and the length of the FBG, and the Fabry-Perot cavity thickness. At the same time, at least five of these parameters depend differently on temperature, and two parameters also depend on humidity. The slightest change in one or more of these ten parameters will instantly change the position of the transparency window. It must be noted that not all parameters equally contribute to the change of the spectral response shape. The proposed model allows to study these phenomena in detail.

Several videos describing the evolution of the spectrum shape of the combined fiber optic sensor depending on variations of its parameters can be found in the supplementary materials [36], the links are given in Conclusions.

With the change of the refractive index (permittivity) of the polymer film, the spectral position of the resonance does not change, which is due to the fact that the period of the fiber Bragg grating remains unchanged, the Bragg-Wulff conditions are preserved, which ensures the constancy of the central wavelength of the FBG reflection spectrum. At the same time, the variation of the polymer permittivity leads to the shift of the Fabry-Perot reflection spectrum. The appearance of the transparency window in the FBG spectrum depends on the relative position of the FBG and the Fabry-Perot cavity spectra. In the Video 1 [36], it can be seen that the transparency window does not appear in the FBG reflection spectrum when the period (the central wavelength) of the Bragg grating is small. As the period (or the central wavelength of the FBG) increases, a transparency window slowly appears in the reflection spectrum. Therefore, we can conclude that the shape of the spectral response depends on the mutual ratio of the Bragg and the Fabry-Perot resonant frequencies.

4. Conclusions

The presented mathematical model can be used as a digital twin of a combined fiber optic sensor. Using the presented mathematical model and the experimental data, we could find the simple asymmetric Fano-type resonance in an optical fiber as a result of superposition of two wave resonance

processes. The similarity of the simulated and the real-life combined sensor spectra is demonstrated. The dependence of the spectral shape of this resonance on the parameters of the sensor structure is discussed. However, it is established that the resonance shape ultimately depends on the mutual ratio of the Bragg and the Fabry-Perot resonant frequencies. It is shown that the sensor with asymmetric Fano-type resonance can provide promising opportunities in fiber-optic sensing.

It must be noted that the development of the proposed combined sensor requires the involvement of specialists from several branches of science. The mathematical model introduced in the current paper makes it possible to carry out the first stage of such development. The model enables high-fidelity simulation of the spectral response of the proposed combined structure. At the same time, the spectral response of this sensitive element depends on at least twelve independent parameters.

In this work, instead of proposing a specific implementation of the sensing element, we give a complete description of the mathematical model that allows one to determine all necessary parameters for any implementation of the sensor tailored to each specific task. For example, when the fiber-optic structure is used as a gas concentration sensor, its sensitivity is determined by dependence of the refractive index (permittivity and permeability) of the polymer material on the environmental gas concentration, temperature and humidity. Moreover, the choice of the specific polymer must be made depending on the type of gas under test.

The task of choosing or synthesizing a polymer material, the dielectric constant of which changes reversibly depending on the concentration of the gas under test, is a separate and fairly complex problem that can be solved by chemists. By performing the simulations using the proposed model, it is possible to determine the required characteristics of the polymer film, namely its permittivity and permeability, and establish the necessary limits of their variations depending on the required measurement range. After that, on the basis of the selected parameters, the task of the synthesis of a material with the required characteristics is assigned.

The video files are provided as supplementary materials [36]. The videos contain the spectrum dynamics with variations of the FBG period (Video 1), environmental temperature (Video 2), refractive index of the Fabry-Perot cavity (Video 3) and the environment (Video 4). The authors are ready for collaboration with laboratories engaged in similar research.

Acknowledgements

The work was supported by the Ministry of Science and Higher Education under the “Priority Q2 2030” program and by the Ministry of Education and Science of Russian Federation Reg. R&D number AAAA-A20-120122490071-1 (Agreement No. 075-03-2020-051, Topic No. fzsu-2020-0020).

References

[1] M.F. Limonov, M.V. Rybin, A.N. Poddubny, Y.S. Kivshar, Fano resonances in photonics, Nature Photon 11 (2017) 543–554, https://doi.org/10.1038/nphoton.2017.142.
[2] P. Chen, Y. Dai, D. Zhang, X. Wen, M. Yang, Cascaded-cavity fabry-perot interferometric gas pressure sensor based on vernier effect, Sensors 18 (2018) 3677, https://doi.org/10.3390/s18113677.
[3] X. Chen, C. Chardin, K. Makles, C. Caër, S. Chua, R. Braive, I. Robert-Philip, T. Briant, P.-F. Cohadon, A. Heidmann, T. Jacqmin, S. Deléglise, High-finesse Fabry–Perot cavities with bidimensional Si_3N_4 photonic-crystal slabs, Light Sci. Appl. 6 (2017) e16190, https://doi.org/10.1038/lsa.2016.190.
[4] Z. Li, Y.-X. Zhang, W.-G. Zhang, L.-X. Kong, T.-Y. Yan, P.-C. Geng, B. Wang, High-sensitivity gas pressure fabry–perot fiber probe with micro-channel based on vernier effect, J. Lightwave Technol. 37 (2019) 3444–3451, https://doi.org/10.1109/JLT.2019.2917062.
[5] S. Guo, C. Hu, H. Zhang, Unidirectional ultrabroadband and wide-angle absorption in graphene-embedded photonic crystals with the cascading structure comprising the Octonacci sequence, J. Opt. Soc. Am. B 37 (2020) 2678, https://doi.org/10.1364/JOSAB.399048.
[6] Y. Ma, H. Zhang, H. Zhang, T. Liu, W. Li, Properties of unidirectional absorption in one-dimensional plasma photonic crystals with ultra-wideband, Appl. Opt. 57 (2018) 8119, https://doi.org/10.1364/AO.57.008119.
[7] B.-F. Wan, Z.-W. Zhou, Y. Xu, H.-F. Zhang, A theoretical proposal for a refractive index and angle sensor based on one-dimensional photonic crystals, IEEE Sensors J 21 (2021) 331–338, https://doi.org/10.1109/JSEN.2020.3013289.
[8] S.F.H. Correia, P. Antunes, E. Pecoraro, P.P. Lima, H. Varum, L.D. Carlos, R.A.S. Ferreira, P.S. André, Optical fiber relative humidity sensor based on a FBG with a di-ureasil coating, Sensors 12 (2012) 8847–8860, https://doi.org/10.3390/s120708847.
[9] R.C.S.B. Allil, . M.M., B.A., F.V.B. de Nazar, Application of fiber bragg grating sensors in power industry, in: C. Cuadrado-Laborde, eds., Current Trends in Short- and Long-Period Fiber Gratings, IntechOpen, London, United Kingdom. (2013), pp. 133–166, https://doi.org/10.5772/54148.
[10] G.P. Agrawal, S. Radic, Phase-shifted fiber Bragg gratings and their application for wavelength demultiplexing, IEEE Photon. Technol. Lett. 6 (1994) 995–997, https://doi.org/10.1109/68.313074.
[11] H.M. El-Gammal, E.-S.A. El-Badawy, M.R.M. Rizk, M.H. Aly, A new hybrid FBG with a π-shift for temperature sensing in overhead high voltage transmission lines, Opt. Quant. Electron. 52 (2020) 1–24, https://doi.org/10.1007/s11082-019-2171-7.
[12] Q. Zhang, N. Liu, T. Fink, H. Li, W. Peng, M. Han, Fiber-optic pressure sensor based on π-phase-shifted fiber bragg grating on side-hole fiber, IEEE Photon. Technol. Lett. 24 (2012) 1519–1522, https://doi.org/10.1109/LPT.2012.2207715.
[13] C.E. Campanella, F.D. Leonardis, L. Mastronardi, P. Malara, G. Gagliardi, V.M.N. Passaro, Investigation of refractive index sensing based on Fano resonance in fiber Bragg grating ring resonators, Opt. Express, OE. 23 (2015) 14301–14313, https://doi.org/10.1364/OE.23.014301.

[14] O.G. Morozov, I.I. Nureev, A.Z. Sahabutdinov, R.R. Gubaidullin, G.A. Morozov, Problem of fano resonance characterization in ring π-shift fiber bragg grating biosensors, in: 2019 Systems of Signal Synchronization, Generating and Processing in Telecommunications (SYNCHROINFO),, 2019, pp. 1–6, https://doi.org/10.1109/SYNCHROINFO.2019.8814206.
[15] G. Wamg, Q. Shi, F. Chen, Y. Yu, Gas sensor based on multiple Fano resonances in metal-insulator-metal waveguide resonator system, J. Optoelectron. Adv. Mater. 24 (2022) 323–331.
[16] F. Chen, H. Zhang, L. Sun, J. Li, C. Yu, Temperature tunable Fano resonance based on ring resonator side coupled with a MIM waveguide, Opt Laser. Technol. 116 (2019) 293–299, https://doi.org/10.1016/j.optlastec.2019.03.044.
[17] Z. Shen, M. Du, High-performance refractive index sensing system based on multiple Fano resonances in polarization-insensitive metasurface with nanorings, Opt Express 29 (2021) 28287, https://doi.org/10.1364/OE.434059.
[18] C.E. Campanella, F. De Leonardis, V.M.N. Passaro, Performance of Bragg grating ring resonator as high sensitivity refractive index sensor, in: 2014 Fotonica AEIT Italian Conference on Photonics Technologies, 2014, pp. 1–4, https://doi.org/10.1109/Fotonica.2014.6843873.
[19] C. Ciminelli, C.E. Campanella, F. Dell'Olio, M.N. Armenise, Fast light generation through velocity manipulation in two vertically-stacked ring resonators, Opt Express 18 (2010) 2973–2986, https://doi.org/10.1364/OE.18.002973.
[20] I. Teraoka, A hybrid filter of Bragg grating and ring resonator, Opt Commun. 339 (2015) 108–114, https://doi.org/10.1016/j.optcom.2014.11.077.
[21] K. McGarvey-Lechable, P. Bianucci, Maximizing slow-light enhancement in one-dimensional photonic crystal ring resonators, Opt Express 22 (2014) 26032–26041, https://doi.org/10.1364/OE.22.026032.
[22] S. Nic Chormaic, Y. Wu, J.M. Ward, Whispering gallery mode resonators as tools for non-linear optics and optomechanics, in: A.V. Kudryashov, A.H. Paxton, V.S. Ilchenko, eds., Laser Resonators, Microresonators, and Beam Control XIV, SPIE, San Francisco, California, USA. (2012), p. 82361K, https://doi.org/10.1117/12.906665.
[23] P. Ji, Q. Shi, L. Zheng, G. Wang, F. Chen, High sensitivity plasmonic refractive index and temperature sensor based on square ring shape resonator with nanorods defects, Opt. Quant. Electron. 54 (2022) 184, https://doi.org/10.1007/s11082-022-03572-4.
[24] P.-H. Merrer, O. Llopis, G. Cibiel, Laser stabilization on a fiber ring resonator and application to RF filtering, IEEE Photon. Technol. Lett. 20 (2008) 1399–1401, https://doi.org/10.1109/LPT.2008.927877.
[25] B. Wan, H. Zhang, P. Wang, Nonreciprocal absorber with a narrow band of angular polarization sensitive regions based on a quasi-periodic structure, Opt. Lett. 46 (2021) 1934–1937, https://doi.org/10.1364/OL.419107.
[26] O. Morozov, Y. Tunakova, S.M.R.H. Hussein, A. Shagidullin, T. Agliullin, A. Kuznetsov, B. Valeev, K. Lipatnikov, V. Anfinogentov, A. Sakhabutdinov, Addressed combined fiber-optic sensors as key element of multisensor greenhouse gas monitoring systems, Sensors 22 (2022) 4827, https://doi.org/10.3390/s22134827.
[27] A.Z. Sakhabutdinov, V.I. Anfinogentov, O.G. Morozov, Yu.A. Tunakova, M.P. Danilaev, I.I. Nureev, A.A. Kuznetcov, K.A. Lipatnikov, A.R. Shagidullin, K.G. Karimov, S.M.R.H. Hussein, B.I. Valeev, Digital twin of the Fabry-Perot sensor for greenhouse gas concentration monitoring, Electronics, Photonics and Cyberphysical Systems 2 (2022) 54–66.
[28] S.M.R.H. Hussein, A.Zh. Sakhabutdinov, O.G. Morozov, V.I. Anfinogentov, J.A. Tunakova, A.R. Shagidullin, A.A. Kuznetsov, K.A. Lipatnikov, A.R. Nasybullin, Applicability limits of the end face fiber-optic gas concentration sensor, based on Fabry-Perot interferometer, Karbala International Journal of Modern Science 8 (2022) 339–355, https://doi.org/10.33640/2405-609X.3243.
[29] S. Poeggel, D. Duraibabu, K. Kalli, G. Leen, G. Dooly, E. Lewis, J. Kelly, M. Munroe, Recent improvement of medical optical fibre pressure and temperature sensors, Biosensors 5 (2015) 432–449, https://doi.org/10.3390/bios5030432.
[30] M. Yamada, K. Sakuda, Analysis of almost-periodic distributed feedback slab waveguides via a fundamental matrix approach, Appl. Opt., AO. 26 (1987) 3474–3478, https://doi.org/10.1364/AO.26.003474.
[31] Raman Kashyap, Fiber Bragg Gratings, second ed., Acdemic Press, Burlington, MA. (2009).
[32] C.E. Campanella, P. Malara, C.M. Campanella, F. Giove, M. Dunai, V.M.N. Passaro, G. Gagliardi, Mode-splitting cloning in birefringent fiber Bragg grating ring resonators, Opt. Lett., OL. 41 (2016) 2672–2675, https://doi.org/10.1364/OL.41.002672.
[33] C.E. Campanella, A. Giorgini, S. Avino, P. Malara, R. Zullo, G. Gagliardi, P.D. Natale, Localized strain sensing with fiber Bragg-grating ring cavities, Opt. Express, OE. 21 (2013) 29435–29441, https://doi.org/10.1364/OE.21.029435.
[34] W. Liang, L. Yang, J.K. Poon, Y. Huang, K.J. Vahala, A. Yariv, Transmission characteristics of a Fabry-Perot etalon-microtoroid resonator coupled system, Opt. Lett., OL. 31 (2006) 510–512, https://doi.org/10.1364/OL.31.000510.
[35] D. Yang, Y. Liu, Y. Wang, T. Zhang, M. Shao, D. Yu, H. Fu, Z. Jia, Integrated optic-fiber sensor based on enclosed EFPI and structural phase-shift for discriminating measurement of temperature, pressure and RI, Opt Laser. Technol. 126 (2020) 106112, https://doi.org/10.1016/j.optlastec.2020.106112.
[36] A.Zh. Sakhabutdinov, Airat Zh. Sakhabutdinov, Spectrum of the combined fiber bragg sensors and fabry-pero interferometer, professor airat Zh. Sakhabutdinov, my blog. http://phdkot.blogspot.com/2022/10/combined-fiber-bragg-aensors.html#more, 2022. (accessed October 29 2022).